nature communications

Article

https://doi.org/10.1038/s41467-025-67000-3

Chiral hypervalent iodine catalyzed stereoselective skeletal editing of pyrimidine fused heterocycles

Received: 13 January 2025

Accepted: 20 November 2025

Published online: 04 December 2025

Check for updates

Wen-Wu Sun ✉, Yi-Bing Xie & Bin Wu ✉

In the realm of molecular construction, the skeletal editing techniques of heterocyclic compounds demonstrate unique efficiency, particularly in synthesizing molecular structures that are challenging to obtain through traditional synthetic methods. Compared to the ring-contraction reaction of saturated nitrogen heterocycles and aryl rings, the site selectivity and stereoselective skeletal editing of pyrimidine fused heterocycles remain relatively underdeveloped. Here we report a chiral hypervalent iodine(III)-catalyzed skeletal editing of pyrimidine moieties within polynitrogen heterocycles, which efficiently produces optically pure multi-substituted imidazoline rings. The reaction demonstrates exceptional functional group tolerance, as shown by the ring contraction of diverse polynitrogen heterocycles and the late-stage functionalization of M_1G-*d*R and its analogues, including nucleosides, nucleotides, and oligonucleotides. Density functional theory calculations explore the details of the mechanism and the factors that determine the reaction's stereoselectivity.

Fused nitrogen heterocyclic compounds have received increasing attention in recent decades due to their significant value in the field of medicine[1,2]. The physicochemical properties of these compounds are significantly influenced by the type and size of the ring structure, as well as the substituent groups on the core skeleton[3]. Particularly, quinazolinones and purines, as key structural motifs in many natural products and bioactive compounds[4,5], often exhibit novel physicochemical or biological properties when added with an additional ring[6]. Studies have shown that 2D tricyclic derivatives exhibit enhanced fluorescence properties compared to their 2D bicyclic parent compounds, but with reduced bioactivity (Fig. 1a)[7–9]. In contrast, their 3D tricyclic derivatives exhibit superior pharmacokinetic properties and pharmacological activity, in line with the "escape from flatland" strategy (Fig. 1a)[10–13]. Furthermore, structure-activity relationship studies have confirmed that optically pure compounds possess significantly enhanced bioactivity compared to their racemic counterparts[14,15]. Consequently, the synthesis of chiral semisaturated aza-heterocycles has remained a hot topic in organic synthesis. Traditional synthetic methods rely on cyclization and annulation reactions[10,16,17], which often involve multi-step reaction sequences, pre-functionalized starting materials, and/or harsh reaction conditions. Direct dearomatization of heteroaromatics is an efficient strategy for constructing semisaturated aza-heterocycles, but the reported methods primarily involve electron-rich indoles[18]. Methods for directly converting electron-deficient aza-fused heterocycles into chiral semisaturated aza-heterocycles are rarely reported[19,20].

The skeletal editing strategy is designed to generate reactive intermediates by disrupting the inherent molecular framework, followed by reconfiguration, thereby facilitating swift and facile alterations to the core structure[21–26]. This approach serves as a potent instrument for the rapid and efficient development of drug candidates within the field of medicinal chemistry[27–34]. Among these, the transformation of a three-dimensional (3D) aliphatic six-membered ring into a 3D aliphatic five-membered ring is particularly well-advanced (Fig. 1b)[35–38]. Notably, the photoinduced ring-rearrangement of saturated heterocycles, as recently reported by Sarpong's group, has marked a significant advancement in this area[39,40]. The strategies for skeletal editing of two-dimensional (2D) aromatic six-membered rings to 2D aromatic five-membered rings have also been rapidly evolving (Fig. 1b)[21,35]. Harran[41,42], Zheng[43], and Fu[44] have reported innovative

School of Pharmaceutical Sciences, South-Central Minzu University, Wuhan, China. ✉e-mail: wenwusun@scuec.edu.cn; 2015084@mail.scuec.edu.cn

https://doi.org/10.1038/s41467-025-67000-3

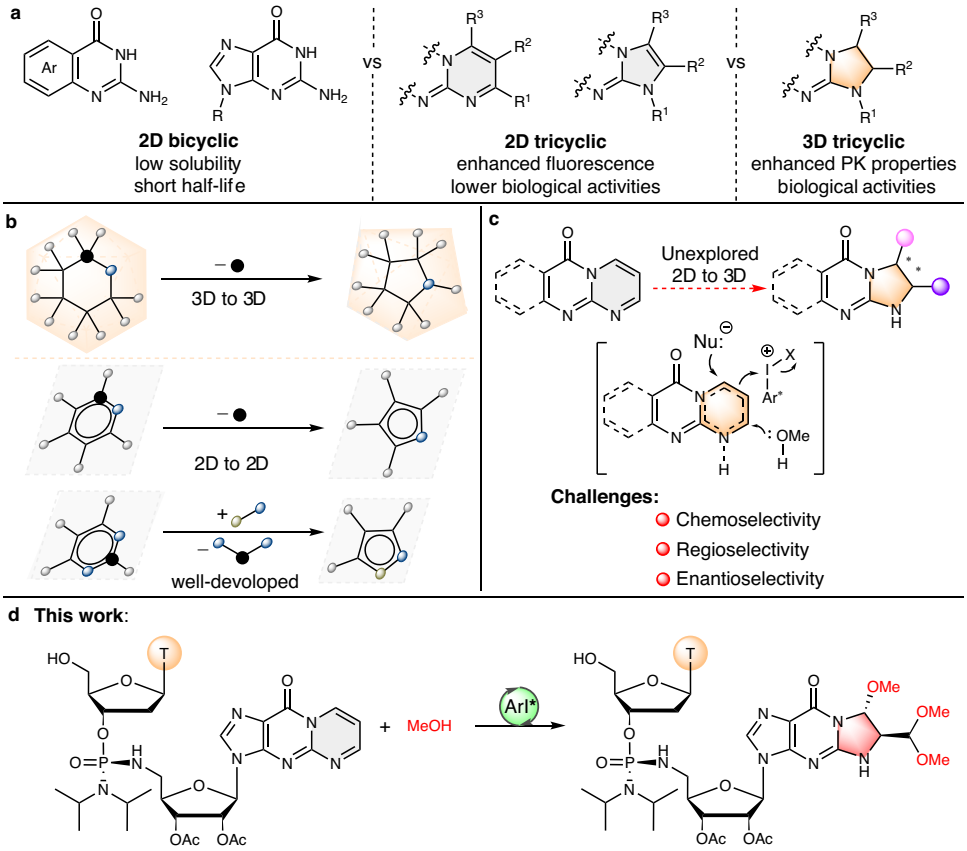

Fig. 1 | Development of stereoselective skeleton editing of polynitrogen heterocycles. a Advantages of semi-saturated tricyclic nucleosides in pharmacokinetic properties or biological properties. **b** Ring contraction reactions: from 3D aliphatic six-membered ring to 3D aliphatic five-membered ring; from 2D aromatic six-membered ring to 2D aromatic five-membered ring. **c** Design and challenges of stereoselective ring contraction from a 2D six-membered ring to a 3D five-membered ring. **d** This work: stereoselective skeletal editing of fused polyazapolycycles.

methods for the transformation of pyridine structures into pyrrole and pyrazole frameworks, respectively. Levin's group also introduced a novel approach to prepare indole compounds by removing carbon from quinoline skeleton through photochemical reaction[45,46]. Furthermore, McNally[47], Sarpong[48] and Fu[49] have independently reported effective strategies for the synthesis of pyrazole and oxazole scaffolds through the deconstruction-reconstruction of pyrimidine skeletons. Despite these studies' significant contributions to scientific progress in the field, asymmetric skeletal editing methods for aza-heterocycles are limited, with only You[50] and Bi's[51] groups reporting asymmetric annulation reactions of indoles. Selective editing of pyrimidine-fused aza-heterocycles, particularly the stereoselective ring contraction rearrangement of 2D aza-heterocycles to chiral 3D aza-heterocycles, remains an underexplored area.

Chiral hypervalent iodine reagents are pivotal tools in organic synthesis, increasingly playing a significant role in the field of asymmetric synthesis[52]. Recent research on chiral hypervalent iodine reagents has made remarkable progress, particularly in applications such as asymmetric dearomatization, α-functionalization of carbonyls, difunctionalization of alkenes, alkene oxidation rearrangements, and oxidative coupling reactions[52,53]. However, the electron-deficient nature, high polarity, poor solubility of pyrimidine-fused heterocycles, and the presence of multiple reactive sites[54–56] pose significant challenges to the high chemo-, regio-, and enantioselective ring contraction rearrangement of pyrimidine catalyzed by chiral hypervalent iodine. Building on our previous work with hypervalent iodine mediated dialkoxylation of electron-rich indole compounds[57], we hypothesized that the introduction of a methoxy group into the electron-deficient pyrimidine ring, followed by rearrangement with hypervalent iodine, could be a viable approach (Fig. 1c). The in situ introduction of the methoxy group not only alters the electronic properties of the compound but also enhances its solubility. Moreover, the methoxy group is an important pharmacophore group that plays a significant role in ligand-target interactions, the physicochemical properties of drugs, and ADME (absorption, distribution, metabolism, and excretion) characteristics[58]. We herein report a chiral hypervalent iodine(III)-catalyzed ring contraction rearrangement of pyrimidine moieties to form multi-substituted imidazolidine rings, successfully achieving a highly chemo-, regio- and stereo-selective transformation from 2D nitrogen heterocycles to fused 2D/3D nitrogen heterocycles (Fig. 1d). Compared with existing methods for imidazoline synthesis[59–61], this approach exhibits superior atom economy, step economy, and substrate versatility.

Results and discussion

Reaction design and optimization

To initiate this study, tricyclic quinazolone **1a** was selected as a model substrate for investigating the asymmetric ring-contraction reaction catalyzed by chiral hypervalent iodine. The utilization of chiral iodoarene **3a** as a precatalyst and MeOH as both reagent and solvent did not lead desired result (Fig. 2, entry 1). Consequently, alternative chiral iodoarene precursors with distinct backbones were explored. Encouragingly, when chiral iodoarene **4a** was employed, the desired compound **2a** was obtained with excellent stereoselectivity, albeit a poor enantioselectivity, yielding 66% (Fig. 2, entry 3). To enhance the reaction outcome, the effect of acid additives was investigated (Fig. 2, entries 5-8). Employing TfOH resulted in an increased yield of compound **2a**, reaching 84%. Notably, replacing MeOH with DCM as the

https://doi.org/10.1038/s41467-025-67000-3

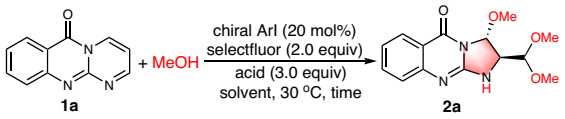

entry	chiral ArI	acid	solvent	time (h)	yield (%), *ee* (%), d.r. of **2a**
1	**3a**	TFA	MeOH	20	-, -, -
2	**3b**	TFA	MeOH	20	-, -, -
3	**4a**	TFA	MeOH	20	66, 25, 20:1
4	**4b**	TFA	MeOH	20	80, 8, 20:1
5	**4a**	-	MeOH	12	57, 20, 20:1
6	**4a**	TfOH	MeOH	12	84, 26, 20:1
7	**4a**	$BF_3.Et_2O$	MeOH	12	66, 14, 20:1
8	**4a**	BF_3.THF	MeOH	12	40, 18, 20:1
9	**4a**	TfOH	DCM	48	80, 56, 20:1
10	**4c**	TfOH	DCM	36	88, 94, 20:1
11	**5a**	TfOH	DCM	24	86, 82, 20:1
12	**5b**	TfOH	DCM	36	88, 76, 20:1
13	**5c**	TfOH	DCM	24	89, 97, 20:1

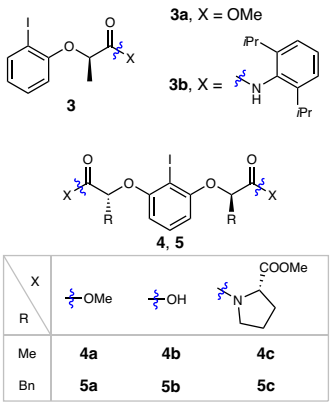

Fig. 2 | Optimization of the reaction conditions. Reaction conditions: **1** (0.1 mmol, 1.0 equiv), MeOH (0.4 mL, 99.0 equiv), chiral ArI (20 mol%), selectfluor (2.0 equiv), acid (3.0 equiv), solvent (4.0 mL) at 30 °C of x h. Yield of isolated product. The enantiomeric excess (*ee*) values were determined by HPLC. The diastereomeric ratio (d.r.) was determined by ^{1}H NMR spectroscopy of the crude reaction mixture.

solvent further enhanced the enantioselectivity to 56% ee (Fig. 2, entry 9). Subsequently, additional investigations focused on exploring the effectiveness of different chiral iodoarenes. Using the (*S*)-proline-derived chiral organoiodine **5c**, the desired compound **2a** was obtained with excellent stereoselectivity, exhibiting a yield of 89% and an impressive enantioselectivity of 97% ee (Fig. 2, entry 13). Regrettably, the expansion to other nucleophiles did not yield the expected results. The addition of benzylamine triggered the decomposition of starting material **1a**, while nucleophiles such as acetic acid, thiophenol, and methyl acetoacetate failed to induce rearrangement, with most of **1a** being recovered (see ESI, Table S5).

Substrate scope of pyrimidine fused heterocycles and alcohols

With the optimized reaction conditions established, the substrate scopes and limitations of this protocol were explored (Fig. 3). The quinazolinone bearing different groups on the phenyl ring afforded the polysubstituted fused-ring guanidines (**2a**-**2l**) with moderate to good yields (35-89%), excellent enantioselectivities (91-99% ee) and diastereoselectivities (>20:1 d.r.). **2a** was synthesised in 73% yield and 98% ee in a 1 mmol scale reaction. The absolute configuration of products **2a** and **2 f** was unambiguously confirmed by single-crystal X-ray diffraction. The polyfluoro-substituted and fused tetracyclic substrates also reacted smoothly, and the ee values of the products **2j**-**2l** were all above 90%. Subsequently, using primary alcohols (MeOH-*d*4, ethanol and cyclopropylmethanol) as nucleophiles, the desired products **6a**-**6c** were obtained in 52-80% yields with up to 97% ee. In addition, the versatility of this synthetic approach for nitrogen-containing bicyclic substrates was investigated. Under standard reaction conditions, two pyrimidine-fused pyrimidines **7a** and **7b** were successfully converted to pyrimidine-fused imidazoline products **8a** and **8b**. The methodology was extended to the synthesis of 5,5-fused bicyclic systems, in particular using triazole-fused pyrimidine **7 d** to produce triazole-fused imidazoline **8 d** in moderate yields and excellent enantioselectivity (93% ee).

Application in late-stage functionalization

Encouraged by the aforementioned experimental results, we intend to apply the developed method to the late-stage functionalization of endogenous nucleoside M_1G-*d*R and its derivatives (Fig. 4). Initially, alkyl-substituted tricyclic nucleosides (ethyl, *n*-butyl and benzyl) were used as substrates, giving the target products **10a**-**10c** in 63-65% yields and 93-95% ee values. Acyclovir, an antiviral drug against herpes simplex virus, and its series of amino acid and peptide-linked derivatives react with TMOP to form M_1G-like acyclic nucleosides[62]. These substrates also underwent selective skeletal editing of the pyrimidine ring under standard conditions, yielding the annulated products **10d**-**10i** with good yields, high diastereoselectivity and excellent enantioselectivity (>90% ee). The method developed can be directly applied to the late-stage functionalization of unprotected M_1G-*d*R **9j** and M_1G-R **9 l**, albeit with less than ideal yields. We have tried changing different chiral columns and mobile phases, as well as derivatising the product, but failed to separate the diastereoisomers by HPLC. Under the standard reaction conditions, the Obz-protected derivatives of M_1G-*d*R **9k** and M_1G-R **9 m** exhibited significantly enhanced reactivity, yielding the desired products **10k** and **10 m** with yields of 28% and 67%, respectively. The tricyclic guanosine derivative with a 5′-position azide substitution also reacted to form the corresponding target product **10n**, with the azide group serving as a reactive site for further structural modification. In nature, nucleosides require activation by kinases to form nucleotides, and modified nucleosides are challenging to phosphorylate in vivo, thus making the late-stage functionalization of nucleotides highly significant. Using the tricyclic nucleotides **9o** and **9p** as substrates, the target products **10o** and **10p** were synthesized under standard conditions. Notably, when the substrates were M_1G-containing oligonucleotides, the desired products **10q** and **10r** were obtained with yields of 18% and 57%, respectively. Compared with their acyclic counterparts, nucleoside, nucleotide, and oligonucleotide substrates performed poorly under identical conditions. We attribute this outcome to the lability of the glycosidic bond, which leads to partial decomposition of the starting material. Attempts to optimize the reaction parameters provided no improvement.

To showcase the synthetic utility of the current methodology, the recycling of chiral catalysts and derivatization reactions of the tricyclic nucleosides were performed (Fig. 5). The chiral catalyst ***re*-5c** was reused and recycled three times with minimal change in the yield and enantiomeric excess of the target product **2a** (Fig. 5a). Compounds **10k** and **10 m** were deprotected to give **10j** and **10 l** in excellent yields. The azide-substituted product **10n** underwent a click reaction with 6-bromo-9-(prop-2-yn-1-yl)–9*H*-purine to afford the triazole-linked oligonucleotide derivative **11** in a 92% yield (Fig. 5b).

https://doi.org/10.1038/s41467-025-67000-3

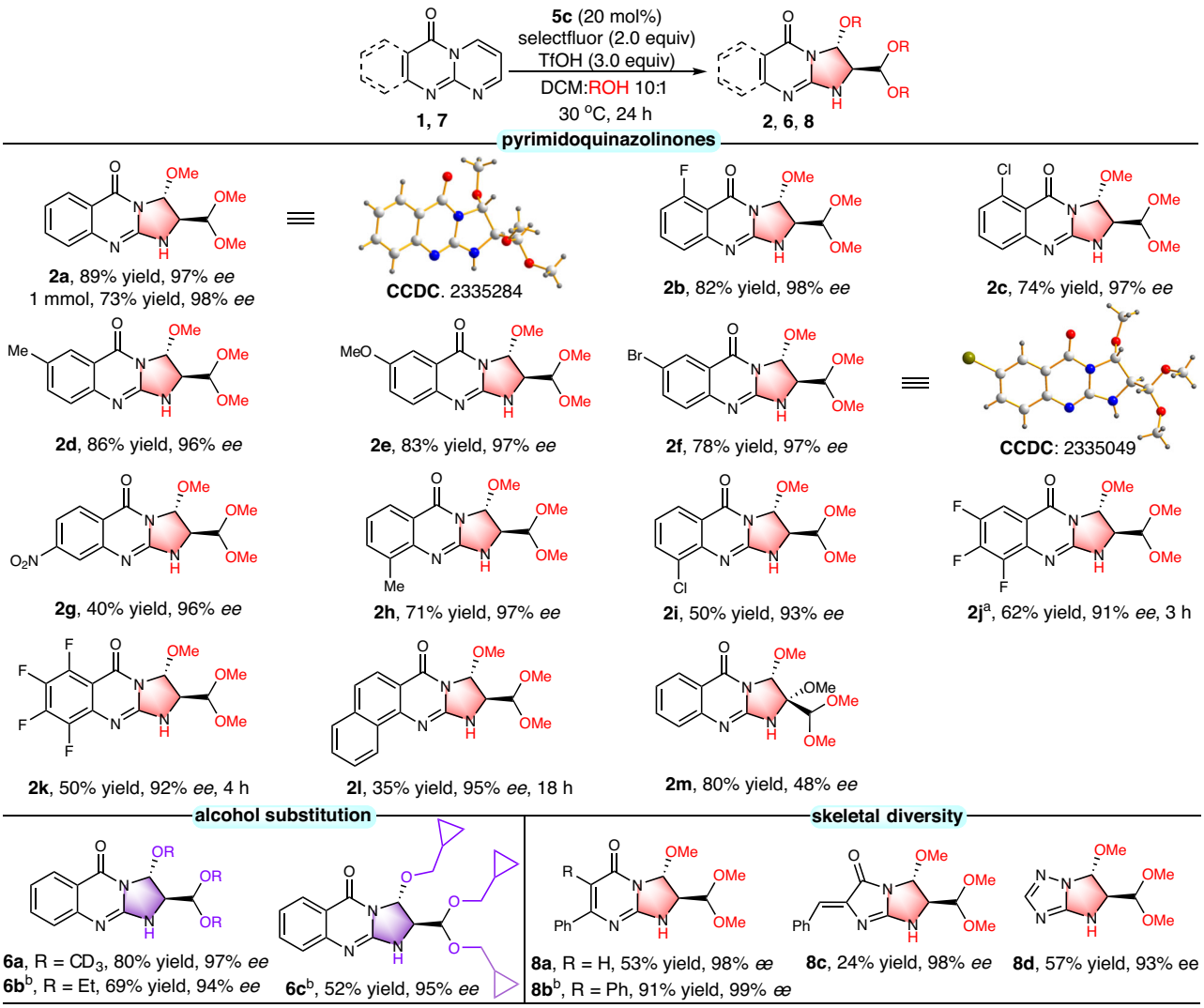

Fig. 3 | Substrate scope of fused polyazapolycycles and alcohols. Reaction conditions: **1** or **7** (0.1 mmol, 1.0 equiv), **5c** (20 mol%), selectfluor (2.0 equiv), TfOH (3.0 equiv), co-solvent DCM:ROH (v/v 10:1, 4.4 mL) at 30 °C. Yield of isolated product. The *ee* values were determined by HPLC. The diastereomeric ratio (d.r.) was determined by ^{1}H NMR spectroscopy of the crude reaction mixture. [a]DCM:MeOH (v/v 3:2, 4.4 mL) was used as solvent. [b]DCM:ROH (v/v 1:1, 4.4 mL) was used as solvent.

Mechanistic considerations

Subsequently, we conducted a preliminary mechanistic investigation of the rearrangement reaction (Fig. 6). Under the standard conditions, pyrido[1,2-a]quinoxaline **12** failed to react, underscoring the pivotal role of the N-1 atom in **1a** in initiating the reaction (Fig. 6a, eq 1). When *m*-CPBA or $PhI(OAc)_2$ were employed as oxidants in place of Selectfluor, *m*-CPBA afforded the product **2a** in 46% yield with 98% ee, whereas $PhI(OAc)_2$ delivered the product **2a** in excellent yield but as a racemate (91% yield, 0% ee). These results suggest that Selectfluor first oxidizes the chiral aryl iodide **5c** to a hypervalent iodine species, and this newly formed catalyst then drives the rearrangement reaction (Fig. 6a, eq 2 and 3). When $PhI(OMe)_2$ was employed directly as the catalyst, ***rac*-2a** could be obtained in 55% yield, indicating that the in-situ-generated $Ar^*I(OMe)_2$ is the active catalytic species (Fig. 6a, eq 4).

Guided by literature precedents[63,64] and the above experimental findings, we elucidated the mechanism by means of DFT calculations (Fig. 6b). First, substrate **1a** adds to the in-situ-generated chiral hypervalent iodine ($Ar^*I(OMe)_2$) through **TS1** to give **Int1**. The transition state **TS1** is 9.2 kcal/mol lower in energy than the **TS1'**, indicating that the S-configured **Int1** is favored (Fig. 6c). Ligand exchange with TfOH then converts **Int1** into **Int2**. In **Int2**, the methoxy group attached to the hydrogenated pyrimidine moiety significantly stabilizes the iodine(III) cation, with an energy 5.5 kcal/mol lower than that of **Int2'**. A syn-addition (**TS2**) of the MeO^- and the hypervalent iodine (Ar^*IOMe) across **Int2** furnishes **Int3**, consistent with Ariafard's observation of facile syn-additions of phenols with MeOH and hypervalent iodine reagents[65]. The low barrier of 5.0 kcal/mol for this step dictates the high chemo-, regio-, and stereoselectivity observed. **Int3** subsequently releases MeO^- to afford **Int4**. The hydropyrimidine unit in **Int4** has three cis-oriented substituents that cause severe steric hindrance, resulting in a highly distorted conformation. Upon rearrangement (**TS3**), this motif transforms into an imidazoline ring. C-2 migrates to an exocyclic position, resulting in the loss of stereochemistry. Meanwhile, C-3 undergoes an intramolecular nucleophilic substitution that inverts its configuration, delivering the *trans*-configured **Int5** and releasing Ar^*I (**4c**). Finally, **Int5** reacts with MeO^- to deliver the product **2a**.

In conclusion, we have developed a highly chem-regio- and stereoselectivity method for the construction of polysubstituted 3D fused-ring guanidines via a chiral hypervalent iodine(III)-catalyzed ring-contraction rearrangement reaction of pyrimidine rings within polynitrogen heterocycles. The application of this method to the late-stage skeletal modification of endogenous nucleoside M_1G-*d*R and its analogues involving serial polyatom changes is demonstrated. To demonstrate its versatility, the scaled-up synthesis, recycling of chiral

https://doi.org/10.1038/s41467-025-67000-3

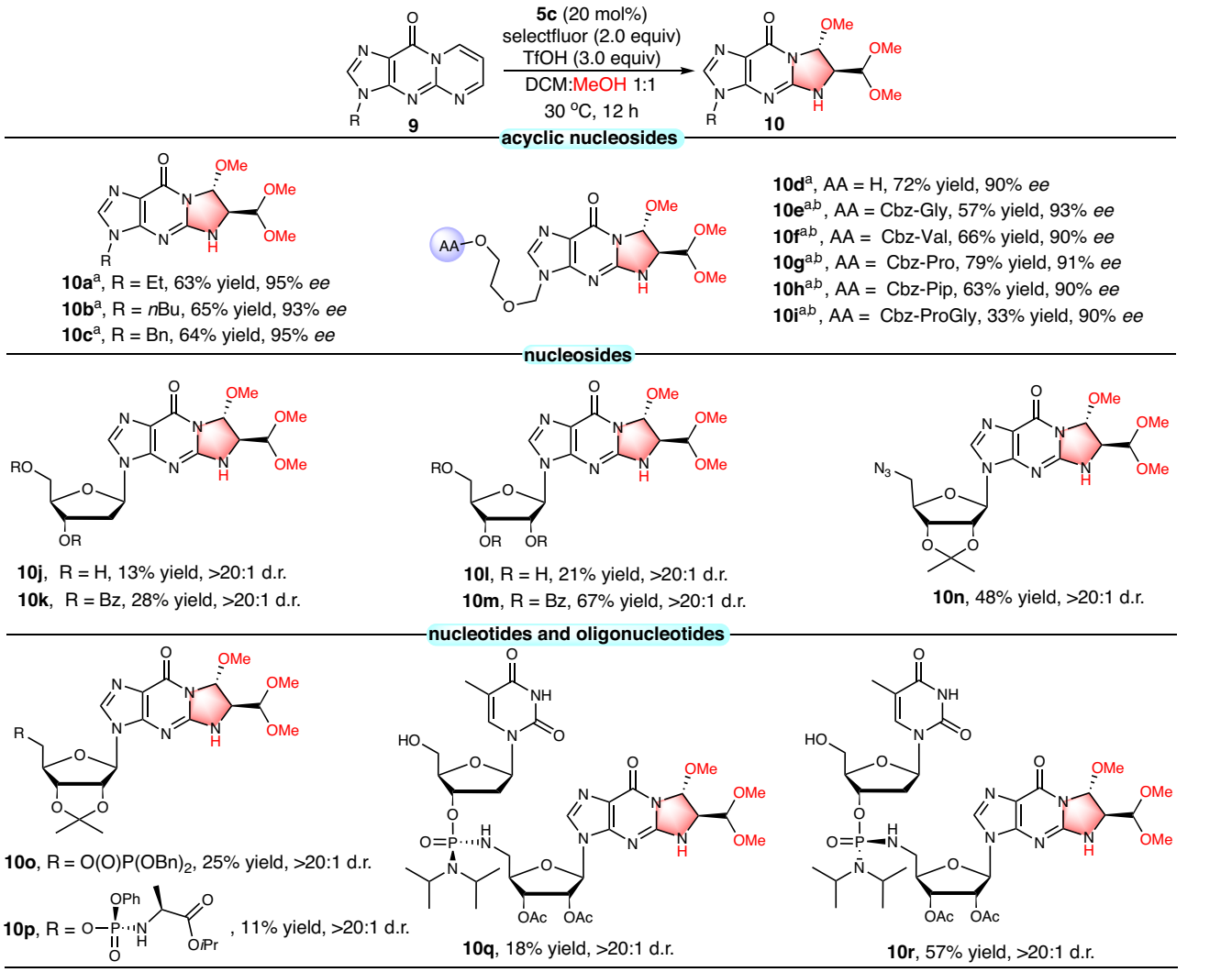

Fig. 4 | Late-stage functionalization of M_1G-*d*R and its analogues. Reaction conditions: **9** (0.1 mmol, 1.0 equiv), **5c** (20 mol%), selectfluor (2.0 equiv), TfOH (3.0 equiv), co-solvent DCM:MeOH (v/v 1:1, 4.4 mL) at 30 °C. Yield of isolated product. The *ee* values were determined by HPLC. The diastereomeric ratio (d.r.) was determined by ^{1}H NMR spectroscopy of the crude reaction mixture. [a]KOH (3.0 equiv) was used as an additive. [b]The *ee* values were determined by HPLC from the hydrolysed product. See Supplementary Information for details.

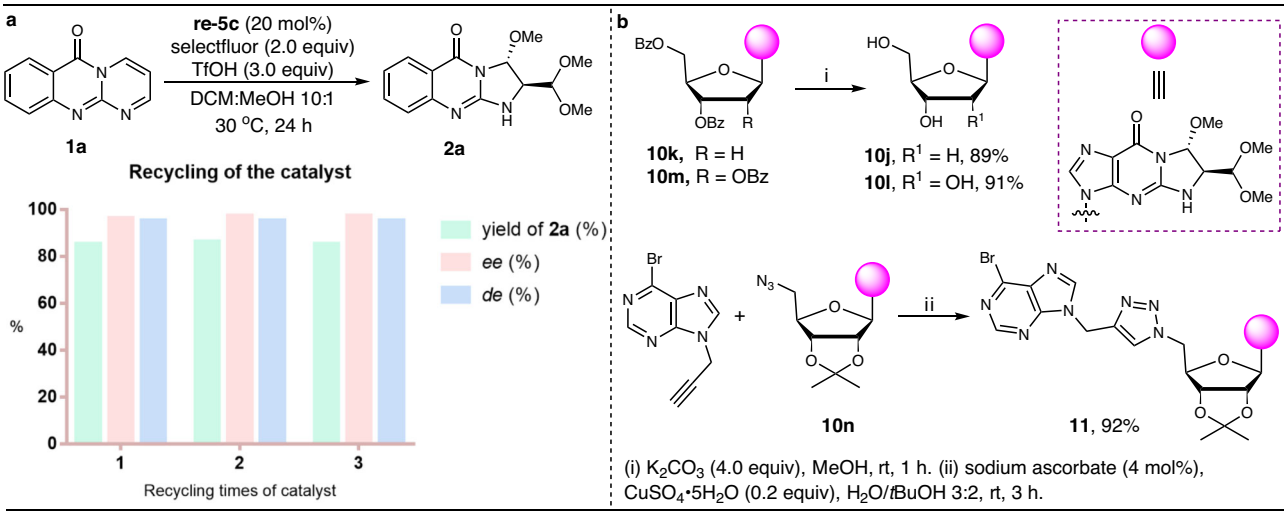

Fig. 5 | Synthetic potentials. a The catalyst recovery and recycling experiments. The scale-up synthesis. **b** The derivatization reaction of tricyclic nucleosides.

https://doi.org/10.1038/s41467-025-67000-3

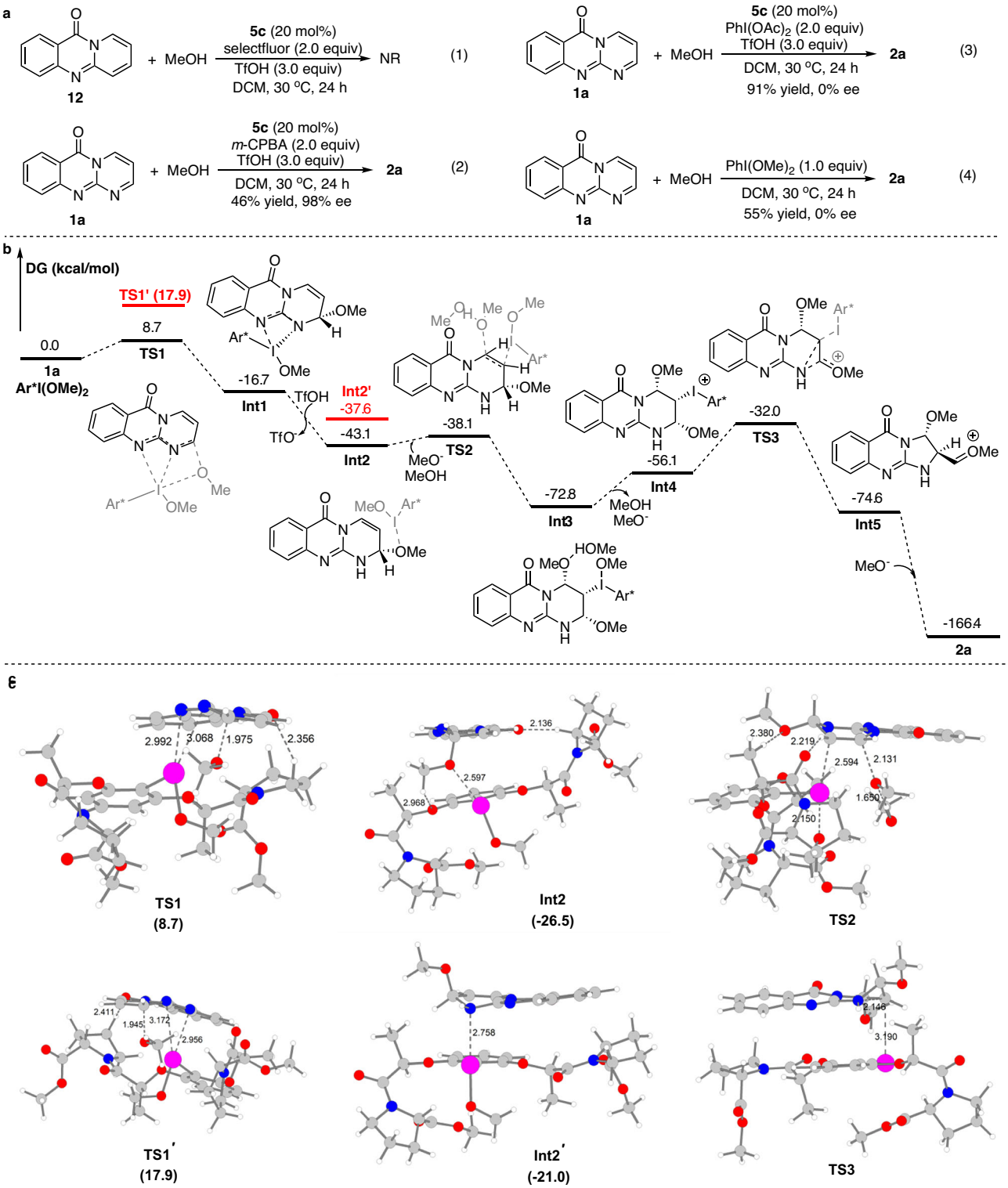

Fig. 6 | Mechanistic observations. a Control experiments. **b** Calculated potential energy profile for Ar*I(OMe)$_2$-catalyzed stereoselective skeletal editing of **1a**. See Supplementary Data 1 for the cartesian coordinates of the optimized structures. **c** Calculated geometries of transition structures and intermediates.

catalysts and derivatization reactions of the tricyclic nucleoside derivatives were successfully carried out.

Methods

General procedure for the synthesis of chiral products

General procedure A. Nitrogen-containing heterocycle (0.1 mmol, 1.0 equiv), **5c** (0.02 mmol, 20 mol%), selectfluor (0.2 mmol, 2.0 equiv) and DCM:ROH (v/v 10:1, 4.4 mL) were added to a screw-capped vial with a magnetic stirrer. TfOH (0.3 mmol, 3.0 equiv) was then rapidly added to the reaction mixture. The vial was tightly sealed and stirred at 30 °C for 3-24 h. The reaction was diluted with DCM and washed with a saturated aqueous solution of $NaHCO_3$. Extract the aqueous phase with DCM. The combined organic phases were dried over anhydrous Na_2SO_4 and concentrated under reduced pressure. The residue was subjected to silica gel chromatography to give target compounds. The enantiomeric excess was determined by HPLC with a chiral column.

General procedure B. KOH (0.3 mmol, 3.0 equiv), **5c** (0.02 mmol, 20 mol%), selectfluor (0.2 mmol, 2.0 equiv) and DCM:MeOH (v/v 1:1, 4.4 mL) were added to a screw-capped vial with a magnetic stirrer. TfOH (0.3 mmol, 3.0 equiv) was then rapidly added to the reaction mixture followed by tricyclic nucleoside (0.1 mmol, 1.0 equiv). The vial was tightly sealed and stirred at 30 °C for 12 h. The reaction was diluted with DCM and washed with a saturated aqueous solution of $NaHCO_3$. Extract the aqueous phase with DCM. The combined organic phases were dried over anhydrous Na_2SO_4 and concentrated under reduced pressure. The residue was subjected to silica gel chromatography to give target compounds. The enantiomeric excess was determined by HPLC with a chiral column.

General procedure C. Tricyclic nucleoside (0.1 mmol, 1.0 equiv), **5c** (0.02 mmol, 20 mol%), selectfluor (0.2 mmol, 2.0 equiv) and DCM:MeOH (v/v 1:1, 4.4 mL) were added to a screw-capped vial with a magnetic stirrer. TfOH (0.3 mmol, 3.0 equiv) was then rapidly added to the reaction mixture. The vial was tightly sealed and stirred at 30 °C for 12 h. The reaction was diluted with DCM and washed with a saturated aqueous solution of $NaHCO_3$. Extract the aqueous phase with DCM. The combined organic phases were dried over anhydrous Na_2SO_4 and concentrated under reduced pressure. The residue was subjected to silica gel chromatography to give target compounds. The enantiomeric excess was determined by HPLC with a chiral column.

Data availability

Crystallographic data for compounds **2a** (CCDC 2335284), **2 f** (CCDC 2335049), and **9q** (CCDC 2347563) are available free of charge from the Cambridge Crystallographic Date Centre. Additional optimization, experimental procedures, characterization of new compounds, and all other data supporting the findings are available in the Supplementary Information and Supplementary Data 1. Data supporting the findings of this manuscript are also available from the corresponding author upon request.

References

1. Kumar, A. et al. Nitrogen containing heterocycles as anticancer agents: a medicinal chemistry perspective. *Pharmaceuticals* **16**, 299 (2023).
2. Marshall, C. M., Federice, J. G., Bell, C. N., Cox, P. B. & Njardarson, J. T. An update on the nitrogen heterocycle compositions and properties of U.S. FDA-approved pharmaceuticals (2013–2023). *J. Med. Chem.* **67**, 11622–11655 (2024).
3. Vitaku, E., Smith, D. T. & Njardarson, J. T. Analysis of the structural diversity, substitution patterns, and frequency of nitrogen heterocycles among U.S. FDA approved pharmaceuticals. *J. Med. Chem.* **57**, 10257–10274 (2014).
4. Li, H., Fu, G. & Zhong, W. Natural quinazolinones: from a treasure house to promising anticancer leads. *Eur. J. Med. Chem.* **245**, 114915 (2023).
5. Motter, J. et al. Purine nucleoside antibiotics: recent synthetic advances harnessing chemistry and biology. *Nat. Prod. Rep.* **41**, 873–884 (2024).
6. Lish, M. S. et al. Pharmacophore establishment and optimization of saturated 1,6-naphthyridine-fused quinazolinones that inhibit meningoencephalitis-causing naegleria fowleri. *J. Med. Chem.* **67**, 18265–18289 (2024).
7. Jahnz-Wechmann, Z., Framski, G., Januszczyk, P. & Boryski, J. Bioactive fused heterocycles: Nucleoside analogs with an additional ring. *Eur. J. Med. Chem.* **97**, 388–396 (2015).
8. Goslinski, T., Golankiewicz, B., De Clercq, E. & Balzarini, J. Synthesis and biological activity of strongly fluorescent tricyclic analogues of acyclovir and ganciclovir. *J. Med. Chem.* **45**, 5052–5057 (2002).
9. Golankiewicz, B. et al. Fluorescent tricyclic analogues of acyclovir and ganciclovir. A structure– antiviral activity study. *J. Med. Chem.* **44**, 4284–4287 (2001).
10. Luise, N. & Wyatt, P. G. Generation of polar semi-saturated bicyclic pyrazoles for fragment-based drug-discovery campaigns. *Chem. Eur. J.* **24**, 10443–10451 (2018).
11. Lovering, F., Bikker, J. & Humblet, C. Escape from flatland: increasing saturation as an approach to improving clinical success. *J. Med. Chem.* **52**, 6752–6756 (2009).
12. Wu, W.-L. et al. Discovery of novel tricyclic heterocycles as potent and selective DPP-4 inhibitors for the treatment of type 2 diabetes. *ACS Med. Chem. Lett.* **7**, 498–501 (2016).
13. Karloff, D. B. et al. Glyoxal caging of nucleoside antivirals toward self-activating, extended-release prodrugs. *J. Am. Chem. Soc.* **146**, 29402–29406 (2024).
14. Seri-Levy, A., West, S. & Richards, W. G. Molecular similarity, quantitative chirality, and QSAR for chiral drugs. *J. Med. Chem.* **37**, 1727–1732 (1994).
15. Kahlon, D. K., Lansdell, T. A., Fisk, J. S. & Tepe, J. J. Structural-activity relationship study of highly-functionalized imidazolines as potent inhibitors of nuclear transcription factor-κB mediated IL-6 production. *Bioorg. Med. Chem.* **17**, 3093–3103 (2009).
16. Long, A., Oswood, C. J., Kelly, C. B., Bryan, M. C. & MacMillan, D. W. C. Couple-close construction of polycyclic rings from diradicals. *Nature* **628**, 326–332 (2024).
17. Twigg, D. G. et al. Partially saturated bicyclic heteroaromatics as an sp^3 -enriched fragment collection. *Angew. Chem. Int. Ed.* **55**, 12479–12483 (2016).
18. Xia, Z. L., Xu-Xu, Q. F., Zheng, C. & You, S. L. Chiral phosphoric acid-catalyzed asymmetric dearomatization reactions. *Chem. Soc. Rev.* **49**, 286–300 (2020).
19. Escolano, M. et al. Recent strategies in the nucleophilic dearomatization of pyridines, quinolines, and isoquinolines. *Chem. Rev.* **124**, 1122–1246 (2024).
20. Anjirwala, S. N. & Patel, S. K. Efficient synthetic strategies for fused pyrimidine and pyridine derivatives: a review. *J. Heterocycl. Chem.* **61**, 1481–1516 (2024).
21. Jurczyk, J. et al. Single-atom logic for heterocycle editing. *Nat. Synth.* **1**, 352–364 (2022).
22. Li, J., Tang, P., Fan, Y. & Lu, H. Skeletal editing of pyrrolidines by nitrogen-atom insertion. *Science* **389**, 275–281 (2025).
23. Wu, F.-P., Tyler, J. L. & Glorius, F. Diversity-generating skeletal editing transformations. *Acc. Chem. Res.* **58**, 893–906 (2025).
24. Wang, Z., Xu, P., Guo, S.-M., Daniliuc, C. G. & Studer, A. C-to-N atom swapping and skeletal editing in indoles and benzofurans. *Nature* **642**, 92–98 (2025).
25. Puriņš, M., Nakahara, H. & Levin, M. D. Bridging the pyridine-pyridazine synthesis gap by skeletal editing. *Science* **389**, 295–298 (2025).
26. Liu, L.-J. et al. Indole-quinoline transmutation enabled by a formal rhodium carbynoid. *Angew. Chem. Int. Ed.* **64**, e202501966 (2025).
27. Zhang, P., Hua, L., Takahashi, T., Jin, S. & Wang, Q. Recent advances in the dearomative skeletal editing of mono-azaarenes. *Synthesis* **56**, 55–70 (2023).
28. Roque, J. B., Kuroda, Y., Göttemann, L. T. & Sarpong, R. Deconstructive diversification of cyclic amines. *Nature* **564**, 244–248 (2018).
29. Reisenbauer, J. C., Green, O., Franchino, A., Finkelstein, P. & Morandi, B. Late-stage diversification of indole skeletons through nitrogen atom insertion. *Science* **377**, 1104–1109 (2022).
30. Kennedy, S. H., Dherange, B. D., Berger, K. J. & Levin, M. D. Skeletal editing through direct nitrogen deletion of secondary amines. *Nature* **593**, 223–227 (2021).
31. Conboy, A. & Greaney, M. F. Synthesis of benzenes from pyridines via N to C switch. *Chem* **10**, 1940–1949 (2024).
32. Woo, J., Stein, C., Christian, A. H. & Levin, M. D. Carbon-to-nitrogen single-atom transmutation of azaarenes. *Nature* **623**, 77–82 (2023).

33. Ma, C., Lindsley, C. W., Chang, J. & Yu, B. Rational molecular editing: a new paradigm in drug discovery. *J. Med. Chem.* **67**, 11459–11466 (2024).
34. Li, E.-Q., Lindsley, C. W., Chang, J. & Yu, B. Molecular skeleton editing for new drug discovery. *J. Med. Chem.* **67**, 13509–13511 (2024).
35. Joynson, B. W. & Ball, L. T. Skeletal editing: Interconversion of arenes and heteroarenes. *Helv. Chim. Acta* **106**, e202200182 (2023).
36. Xu, Y.-A., Xiang, S.-H., Che, J.-T., Wang, Y.-B. & Tan, B. Skeletal editing of cyclic molecules using nitrenes. *Chin. J. Chem.* **42**, 2656–2667 (2024).
37. Hui, C., Craggs, L. & Antonchick, A. P. Ring contraction in synthesis of functionalized carbocycles. *Chem. Soc. Rev.* **51**, 8652–8675 (2022).
38. Tanifuji, R. Skeletal editing: Recent progress on ring-contraction. *J. Syn. Org. Chem. Jpn.* **80**, 778–779 (2022).
39. Jurczyk, J. et al. Photomediated ring contraction of saturated heterocycles. *Science* **373**, 1004–1012 (2021).
40. Kim, S. F. et al. Mechanistic investigation, wavelength-dependent reactivity, and expanded reactivity of *N*-aryl azacycle photomediated ring contractions. *J. Am. Chem. Soc.* **146**, 5580–5596 (2024).
41. Hurlow, E. E. et al. Photorearrangement of [8]–2,6-pyridinophane *N*-oxide. *J. Am. Chem. Soc.* **142**, 20717–20724 (2020).
42. Feng, Z., Allred, T. K., Hurlow, E. E. & Harran, P. G. Anomalous chromophore disruption enables an eight-step synthesis and stereochemical reassignment of (+)-marineosin a. *J. Am. Chem. Soc.* **141**, 2274–2278 (2019).
43. Luo, J., Zhou, Q., Xu, Z., Houk, K. N. & Zheng, K. Photochemical skeletal editing of pyridines to bicyclic pyrazolines and pyrazoles. *J. Am. Chem. Soc.* **146**, 21389–21400 (2024).
44. Xu, K. et al. Synthesis of 2-formylpyrroles from pyridinium iodide salts. *Org. Lett.* **22**, 6107–6111 (2020).
45. Woo, J. et al. Scaffold hopping by net photochemical carbon deletion of azaarenes. *Science* **376**, 527–532 (2022).
46. Woo, J., Zeqiri, T., Christian, A. H., Ryan, M. C. & Levin, M. D. Carbon-atom scavengers enable divergent, selective carbon deletion of azaarenes. *J. Am. Chem. Soc.* **147**, 20120–20131 (2025).
47. Uhlenbruck, B. J. H., Josephitis, C. M., de Lescure, L., Paton, R. S. & McNally, A. A deconstruction-reconstruction strategy for pyrimidine diversification. *Nature* **631**, 87–93 (2024).
48. Bartholomew, G. L., Carpaneto, F. & Sarpong, R. Skeletal editing of pyrimidines to pyrazoles by formal carbon deletion. *J. Am. Chem. Soc.* **144**, 22309–22315 (2022).
49. Li, S. et al. Skeletal editing of 4-arylpyrimidines into diverse nitrogen heteroaromatics via four-atom synthons. *Nat. Commun.* **16**, 7112 (2025).
50. Huang, X.-Y., Xie, P.-P., Zou, L.-M., Zheng, C. & You, S.-L. Asymmetric dearomatization of indoles with azodicarboxylates via cascade electrophilic amination/aza-prins cyclization/phenonium-like rearrangement. *J. Am. Chem. Soc.* **145**, 11745–11753 (2023).
51. Zhang, X. et al. Asymmetric dearomative single-atom skeletal editing of indoles and pyrroles. *Nat. Chem.* **17**, 215–225 (2024).
52. Yoshimura, A. & Zhdankin, V. V. Advances in synthetic applications of hypervalent iodine compounds. *Chem. Rev.* **116**, 3328–3435 (2016).
53. Parra, A. Chiral hypervalent iodines: active players in asymmetric synthesis. *Chem. Rev.* **119**, 12033–12088 (2019).
54. Keder, R., Dvorakova, H. & Dvorak, D. New approach to the synthesis of N^7-arylguanines and N^7-aryladenines. *Eur. J. Org. Chem.* **2009**, 1522–1531 (2009).
55. Deetz, M. J., Malerich, J. P., Beatty, A. M. & Smith, B. D. One-step synthesis of 4(3*H*)-quinazolinones. *Tetrahedron Lett.* **42**, 1851–1854 (2001).
56. Merino, P. *Chemical synthesis of nucleoside analogues*. (John Wiley & Sons, 2013).
57. Chen, N. et al. Hypervalent iodine(III)-mediated umpolung dialkoxylation of *N*-substituted indoles. *J. Org. Chem.* **87**, 12759–12771 (2022).
58. Chiodi, D. & Ishihara, Y. The role of the methoxy group in approved drugs. *Eur. J. Med. Chem.* **273**, 116364 (2024).
59. Liu, H. & Du, D.-M. Recent advances in the synthesis of 2-imidazolines and their applications in homogeneous catalysis. *Adv. Synth. Catal.* **351**, 489–519 (2009).
60. Mehedi, M. S. A. & Tepe, J. J. Recent advances in the synthesis of imidazolines (2009–2020). *Adv. Synth. Catal.* **362**, 4189–4225 (2020).
61. Li, J., Yu, B. & Lu, Z. Chiral imidazoline ligands and their applications in metal-catalyzed asymmetric synthesis. *Chin. J. Chem.* **39**, 488–514 (2021).
62. Deng, T.-T. et al. Synthesis of nucleoside and nucleotide analogues by cyclization of the guanine base with 1,1,3,3-tetramethoxypropane. *Org. Lett.* **24**, 7834–7838 (2022).
63. Zhu, W. et al. Catalytic asymmetric nucleophilic fluorination using $BF_3{\cdot}Et_2O$ as fluorine source and activating reagent. *Nat. Commun.* **12**, 3957 (2021).
64. Zhou, B., Haj, M. K., Jacobsen, E. N., Houk, K. N. & Xue, X. S. Mechanism and origins of chemo- and stereoselectivities of aryl iodide-catalyzed asymmetric difluorinations of beta-substituted styrenes. *J. Am. Chem. Soc.* **140**, 15206–15218 (2018).
65. Ganji, B. & Ariafard, A. DFT mechanistic investigation into phenol dearomatization mediated by an iodine(III) reagent. *Org. Biomol. Chem.* **17**, 3521–3528 (2019).

Acknowledgements

This work was supported by the National Natural Science Foundation of China (21772236 grant to B.W.) and the Fundamental Research Funds for the Central Universities, South-Central Minzu University (CZQ23024 grant to W.-W.S.).

Author contributions

W.-W.S. and B.W. conceived the concept, directed the project; W.-W.S. and Y.-B.X. carried out experimental work. W.-W.S. wrote the paper.

Competing interests

The authors declare no competing interests.

Additional information

Supplementary information The online version contains supplementary material available at https://doi.org/10.1038/s41467-025-67000-3.

Correspondence and requests for materials should be addressed to Wen-Wu Sun or Bin Wu.

Peer review information *Nature Communications* thanks Yan Xiong, and the other, anonymous, reviewers for their contribution to the peer review of this work. A peer review file is available.